


RESEARCH

Open Access



# Toxicity monitoring of solvents, hydrocarbons, and heavy metals using statistically optimized model of luminous *Vibrio* sp. 6HFE

Howaida Hassan<sup>1\*</sup> , Marwa Eltarahony<sup>2</sup>, Gadallah Abu-Elreesh<sup>2</sup>, Hanan M. Abd-Elnaby<sup>1</sup>, Soraya Sabry<sup>3</sup> and Hanan Ghozlan<sup>3</sup>

## Abstract

**Background:** The utilization of bioluminescent bacteria in environmental monitoring of water contaminants considers being a vital and powerful approach. This study aimed to isolate, optimize, and apply luminescent bacteria for toxicity monitoring of various toxicants in wastewater.

**Results:** On the basis of light intensity, strain *Vibrio* sp. 6HFE was initially selected, physiologically/morphologically characterized, and identified using the 16SrDNA gene. The luminescence production was further optimized by employing statistical approaches (Plackett-Burman design and central composite design). The maximum bioluminescence intensity recorded  $1.53 \times 10^6$  CPS using optimized medium containing (g/L), yeast extract (0.2g),  $\text{CaCl}_2$  (4.0),  $\text{MgSO}_4$  (0.1), and  $\text{K}_2\text{HPO}_4$  (0.1) by 2.3-fold increase within 1h. The harnessing of *Vibrio* sp. 6HFE as a bioluminescent reporter for toxicity of organic solvents was examined using a bioluminescence inhibition assay. According to  $\text{IC}_{50}$  results, the toxicity order of such pollutants was chloroform > isoamyl > acetic acid > formamide > ethyl acetate > acetonitrile > DMSO > acetone > methanol. However, among eight heavy metals tested, the bioluminescence was most sensitive to  $\text{Ag}^+$  and  $\text{Hg}^+$  and least sensitive to  $\text{Co}^{2+}$  and  $\text{Ni}^{2+}$ . Additionally, the bioluminescence was inhibited by benzene, catechol, phenol, and penta-chlorophenol at 443.1, 500, 535.1, and 537.4 ppm.

**Conclusion:** *Vibrio* sp. 6HFE succeeded in pollution detection at four different environmental and wastewater samples revealing its efficiency in ecotoxicity monitoring.

**Keywords:** Bioluminescence, *Vibrio*, Sepia, Central composite design, Wastewater, Heavy metals, Hydrocarbons

## Introduction

Water is one of the most important natural renewable resources. It is essential for the viability of all life forms. In addition, it plays a vital role in all human practices such as industrial processes, food production,

agriculture, and fisheries. However, human activities have a negative impact on this precious source. Broadly, there are two sources that lead to water pollution: point and non-point sources [1]. The pollution point sources are direct certain and distinguishable sources as industries effluent, tanker release oil, or factory pipe extending into the water, while non-point sources have various numbers and different origins of contaminants that pollute both surface and groundwater such as urban wastes or runoff from agricultural fields [2]. Accordingly, water pollutants could be classified into

\*Correspondence: hoigher@yahoo.com; drhowaidahassanausten@yahoo.com; dr.howiada.hassan@gmail.com

<sup>1</sup> National Institute of Oceanography and Fisheries (NIOF), Marine Environment Division, Marine Microbiology Lab., Kayet Bay, El-Anfushy, Alexandria, Egypt

Full list of author information is available at the end of the article

organic and inorganic. Organohalides, herbicides, volatile organic compounds, and insecticides, etc., are the most common types of organic pollutants, whereas heavy metals, phosphates, and nitrates from industrial effluents and agriculture drainages consider being inorganic pollutants [3, 4].

Due to the water scarcity issue, it is necessary to preserve the water bodies from contamination introduced by several human anthropogenic activities. Therefore, detection of toxic organic and inorganic pollutants in environmental samples has special importance for human health and the entire ecosystem. Several literatures reported routine monitoring of water quality approaches, including chemical analysis of target toxicants and in situ assessment of indigenous biota [5].

Several limitations faced such methods; hence simple, cheap, and rapid monitoring methods were developed, especially that provide data about overall toxicity. Recently, fish, crustaceans, and algae were employed as toxicity evaluation bioassays. However, time-consuming, large sample volume, and capital intensive are the major problems associated with such organisms [6]. Therefore, the employment of microbial cells in the detection and monitoring of toxicants is advantageous in the discipline of ecotoxicological assessment and also as proper alternatives to traditional analytical methods [6].

The general idea of toxicity bioassay relies mainly on the degree of its glowing intensity either in short term or in long term by examining the change in their growth rate and viability [7]. The general mechanism for bioluminescence could be attained to the luciferase enzyme which plays a vital role in the reduction of flavin mononucleotide (FMN) to FMNH<sub>2</sub>, which subsequently reacts with oxygen and produce 4a-peroxy-flavin. This intermediate compound oxidizes the fatty aldehyde to a stable complex (luciferase-hydroxyflavin) which decomposes slowly and illuminates blue-green light [7, 8]. Remarkably, the first and most bioluminescent bacteria used for this purpose was *Vibrio fischeri*; it has high more sensitivity than other bacterial strains to a wide range of chemicals [7]. The bioluminescence of *V. fischeri* is controlled genetically through the transcription process of lux-operon (the luminescence genes). The lux-operon includes two main transcription components, luxR gene and luxICDABEG operon [7–9].

The main aim of the current study focused on the isolation, characterization, and identification of luminous bacteria and, subsequently, defining the growth medium requirements through the optimization process and ultimately applying the isolated strain in toxicity detection of various toxicants, in environmental samples from the marine aqua system and effluents.

## Materials and methods

### Invertebrate samples

Fresh different marine animals (cuttlefish, octopus, squid, and shrimp) were obtained from Maadia port, Alexandria, Egypt. Comb jellyfish was collected from the Eastern harbor of Alexandria, Egypt.

### Isolation of luminous bacteria and growth conditions

Different portions (eye, under the skin, ink sac, intestinal parts, exoskeleton, inner body, feeding tentacles, fins, and head) of collected marine invertebrates were diluted in saline (0.9%) and spread on selective luminescence agar (LA) medium of the following ingredients: 3.0 ml glycerol, 30.0g sodium chloride, 5.0g yeast extract, 5.0g peptone, 5.0, 2.5g di-potassium hydrogen sulfate, 0.25g magnesium sulfate, 1.0g calcium chloride, and 30.0 agar dissolved in 1L MiliQ water; the initial pH was 7.0 ± 0.1 [10]. The plates were incubated at 30°C for 24h [11–13]. The preliminary screening of bioluminescent colonies was performed visually in dark room. The visible luminous colony was picked and streaked on fresh LA plates for more purification. Luminous isolates were stored in 15% glycerol at –85 °C for further studies.

### Bioluminescence measurement for luminous isolates

Bioluminescence (BL) of the positive candidates was measured at regular time intervals by a luminometer (LUMISTAR, Galaxy, BMG, Germany). The intensity was measured in count per second (CPS). The measurement was done by placing 200 µl of bacterial suspension in the Greiner, Transparent, v-bottom-shaped plate. All readings were recorded in triplicate [14, 15]. The isolate which exhibited the highest emitted light was selected for subsequent identification, characterization, optimization, and application steps.

### Molecular identification of the selected luminous isolate

For identification of the selected luminescent bacterial isolate, the chromosomal DNA was extracted from a freshly prepared culture using the EZ-10 Genomic DNA kit (Bio Basic Inc., USA). The amplification of the 16S rDNA gene was performed using universal forward and reverse primers (27F; 5'AGAGTTTGATCCTGG CTCAG3' and 1429 R, 5'TACGGYTACCTTGTTACG ACTT3. The purified 1500-bp amplicon was subjected to sequencing by the ABI PRISM dye terminator cycle sequencing kit with Amplify Taq DNA polymerase and an Applied Biosystem (Thermo Fisher Scientific, USA). The generated sequence was submitted to the GenBank for obtaining the corresponding accession number. N-BLAST program (National Centre for Biotechnology Information) was used to analyze the sequence and compare its similarity with other sequences in the database.

The software package MEGA-X was used to attain multiple alignment and phylogenetic tree.

**Phenotypic characterization of the selected luminous isolate**

The morphological characteristics for the selected isolate were examined by a scanning electron microscope (JEOL JEM-5300, Japan). Other physiological characteristics were determined through biochemical assays by VITEK 2 Compact System, USA, and BIOMERIEUX, USA.

**Bioluminescence intensity optimization**

The light intensity in fast time reaching with maintaining bioluminescence stability is the main criteria in such step. The experiment setup was conducted in a 96-well sterile tissue culture plate with 10 µl of the bacterial culture (0.5McFarland) of selected strain mixed with 190 µl of sterile broth. The optimization step in this study was carried out through two stages: one — variable at a time design (OVAT) and statistical designs including Plackett-Burman design (PBD) and central composite design (CCD).

**One-variable-at-a-time (OVAT) approach**

The maximum light intensity was examined as a function of temperature (25, 30, and 35°C), agitation (static or shaking), and incubation time. Along the experiments, the bioluminescence value (CPS) and growth (OD<sub>600</sub>) were recorded every hour.

**Screening for the significant factors by PBD**

PBD is a fraction of a two-level factorial design that is dedicated to screen and identify the significant variables influencing luminescence intensity emitted by the selected strain. It examines “n-1” variables with at least “n” trials. Each examined variable is represented at two levels, high (+) and low (–) [16]. According to PBD, the number of (+) is equal to (N + 1)/2 and the number of (–) is equal to (N – 1)/2 in a row. In the present study, a total of 8 (n) variables with two-level concentrations were studied in twelve trials as demonstrated in Table 1. The first-order model representing the Plackett-Burman experimental design is indicated by Eq. 1:

$$Y = \beta_0 + \sum \beta_i X_i \tag{1}$$

where Y is the response or dependent variable (bioluminescence intensity); β<sub>0</sub> is the model intercept and β<sub>i</sub> is the linear coefficient, and X<sub>i</sub> is the level of the studied variable. The significance of each factor depending on its nature (i.e., positive or negative effect on the response) was displayed by the main effect that was concluded from the statistical analysis.

**Table 1** The studied nutritional variables with their high and low values examined in PBD

Variable	Coded values for each variable of the PBD		
	–1	0	1
Glycerol (ml/l)	0.5	3.0	6.0
NaCl (g/l)	10.0	30.0	50.0
Yeast extract (g/l)	1.0	5.0	10.0
CaCl <sub>2</sub> (g/l)	0.0	1.0	2.0
Peptone (g/l)	1.0	5.0	10.0
K <sub>2</sub> HPO <sub>4</sub> (g/l)	0.5	2.5	5.0
MgSO <sub>4</sub> (g/l)	0.0	0.25	0.5
pH	5	7	9

**Table 2** Significant variables and their levels in CCD affecting on luminescence intensity of strain *Vibrio* sp. 6HFE

Variable	Coded levels and trial values				
	–α	–1	0	1	α
Yeast extract (g/l)	0.2	0.5	1	4	8
K <sub>2</sub> HPO <sub>4</sub> (g/l)	0.1	0.3	0.5	2	4
MgSO <sub>4</sub> (g/l)	0.1	0.3	0.5	1	2
CaCl <sub>2</sub> (g/l)	0.5	1	2	3	4

**Central composite design (CCD)**

CCD is devoted to elucidating the interactive effect between luminescent intensity and significant variables; additionally, it predicts their optimal levels [16, 17]. Herein, yeast extract, MgSO<sub>4</sub>, CaCl<sub>2</sub>, and K<sub>2</sub>HPO<sub>4</sub> as significant factors, determined by PBD remarkably affected luminescence intensity, were examined at 5 experimental levels: –α, –1, 0, +1, and + α in a 31-trial matrix. The concentrations of the screened significant factor at each level are illustrated in Table 2.

For statistical calculation, the relationship between the coded and actual values is represented by Eq. 2:

$$X_i = U_i - U_{i0} / \Delta U_i \tag{2}$$

where X<sub>i</sub> is the coded value of the i<sup>th</sup> variable, U<sub>i</sub> is the actual value of the i<sup>th</sup> variable, U<sub>i0</sub> is the actual value of the i<sup>th</sup> variable at the center point, and ΔU<sub>i</sub> is the step change of the variable. The second-order polynomial that describes the relationship between response (luminescence intensity) (Y) viz the significant variables was indicated in Eq.3:

$$Y = \beta_0 + \beta_1 X_1 + \beta_2 X_2 + \beta_3 X_3 + \beta_{11} X_{11} + \beta_{22} X_{22} + \beta_{33} X_{33} + \beta_{12} X_1 X_2 + \beta_{13} X_1 X_3 + \beta_{23} X_2 X_3 \tag{3}$$

where  $Y$  is the predicted response;  $X_1$ ,  $X_2$ , and  $X_3$  are input variables which influence the response variable  $Y$ ;  $\beta_0$  intercept;  $\beta_1$ ,  $\beta_2$ , and  $\beta_3$  linear coefficients;  $\beta_{11}$ ,  $\beta_{22}$ , and  $\beta_{33}$  squared or quadratic coefficients; and  $\beta_{12}$ ,  $\beta_{13}$ , and  $\beta_{23}$  interaction coefficients.

### Statistical analysis

The matrices design of PBD and CCD, data interpretation, and regression modeling of the results from the experiment were statistically analyzed using Minitab 14.0 (Minitab Inc., Pennsylvania, USA), statistical software. The first analytical step for both models involves the analysis of variance (ANOVA), followed by regression analysis. Besides, the plotting profiles of CCD to predict the optimum conditions of each studied variable were also determined. The validation of the optimized model was verified through examining the predicted optimum values and comparing it with basal un-optimized media.

### Toxicity determination via bioluminescence inhibition assay (BIA)

The effect of various pollutants with different concentrations on cellular bioluminescence of the selected strain *Vibrio* sp. 6HFE was tested according to the bioluminescence inhibition assay (BIA). Initially, standard solutions of organic solvents (acetic acid, ethyl acetate, acetone, methanol, chloroform, isoamyl, acetonitrile, formamide, and DMSO), heavy metals ( $\text{NiSO}_4 \cdot 6\text{H}_2\text{O}$ ,  $\text{CuCl}_2 \cdot 2\text{H}_2\text{O}$ ,  $\text{HgCl}_2$ ,  $\text{CoCl}_2 \cdot 6\text{H}_2\text{O}$ ,  $\text{AgNO}_3$ ,  $\text{FeSO}_4 \cdot 7\text{H}_2\text{O}$ ,  $\text{ZnCl}_2$ , and  $\text{K}_2\text{Cr}_2\text{O}_7$ ) and hydrocarbons (benzene, phenol, penta-chlorophenol sodium salt, and catechol) were prepared in HPLC grade sterile water. For bioluminescence assays, 100  $\mu\text{l}$  of each toxicant was added to 100  $\mu\text{l}$  of luminous *Vibrio* sp. 6HFE ( $\text{OD} = 0.4 \sim 4 \times 10^6$  CFU) which was placed in a well of a microtiter plate with uniform mixing. Besides, a control was run in parallel to each toxicity well, which contained bacterial culture and sterile water. Three replicates were performed for each concentration of every toxicant. The microplate was incubated overnight in the luminometer shacked at 25°C. Bioluminescence of the culture and treated wells were measured at regular time intervals by a luminometer (LUMISTAR, Galaxy, BMG, Germany). Finally, the percent of the bioluminescence inhibition (BI %) was determined according to the following equations (4 and 5), where ( $t$ ) is the time in min [18].

$$\text{Bioluminescence (\%)} = \frac{\text{bioluminescence of sample after } t \text{ min}}{\text{bioluminescence of control after } t \text{ min}} \times 100 \quad (4)$$

$$\text{Bioluminescence inhibition (\%)} = 100 - \text{Bioluminescence (\%)} \quad (5)$$

Based on BI%, the pollutant could be classified as non-toxic (0-5% BI%), possibly toxic (5-20% BI%), and

toxic (> 20% BI%) as referred by [18–20]. Additionally, another parameter was taken into consideration which is  $\text{IC}_{50}$ . It is the pollutant concentration which resulted in bioluminescence reduction by 50% after exposure to ( $t$ ) time. It could be obtained from a non-linear regression relationship.

### Application of *Vibrio* sp. 6HFE in pollution detection at environmental water samples

Two industrial discharges (wastewater) from Tiba for food industries at the 2nd industrial Zone and AKSA Company at the 4<sup>th</sup> industrial Zone, New Borg El Arab, Alexandria, in addition to two water samples from seawater of El-Dekheila and El-Max regions, Alexandria, were collected. Samples were filtered and prepared in order to be analyzed for heavy metals using Atomic Absorption spectrometer-S, Series (Thermo Fisher Scientific). For the bioluminescence assays, about 100  $\mu\text{l}$  of each water sample was mixed with 100  $\mu\text{l}$  of a luminous *Vibrio* sp. 6HFE culture in 96-well microtiter plates (Nunc). Consequently, the inoculated plates were subjected for luminescence detection at room temperature as previously described.

## Results and discussion

### Results

#### Isolation and identification of bacterial isolates

Judging from the light intensity of emitting luminescence, bioluminescent colonies were selected and further purified. Out of the twenty-five bacteria isolated from marine animals, only twelve showed obvious glowing with different degrees of bioluminescence as visually observed and then intensity was measured. Table 3 summarizes the visual observation, light intensity of isolates, and their isolation source.

It was observed that isolates occupying the front body part of sepia, octopus, and squid such as the head, eyes, and feeding tentacles showed more intense bioluminescence than those isolated from other body parts (Table 3).

#### Bioluminescent bacteria (BLB) identification and phylogenetic analysis

Based on the highest and the most stable intensity of blue-green light in LA media, the luminescent isolate was designated as SP5, which was chosen for further steps. The isolate was subjected to taxonomic identification via partial 16S rDNA sequences which displayed 94% DNA similarities with the number of species of the genus *Vibrio*. The sequence was deposited in GenBank with accession number MH463249 as *Vibrio* sp. 6HFE. It is affiliated to the phylum Proteobacteria, class gammaproteobacteria, order Vibrionales, and family Vibrionaceae. The phylogenetic tree of *Vibrio* sp. 6HFE was constructed by the neighbor-joining (NJ) method as indicated in Fig. 1.

**Table 3** Sources of bioluminescent bacterial isolates and their bioluminescence

Isolate code	Source	Visual observation	BL intensity (CPS) × 10 <sup>6</sup>
Cr1	Crabs	+	1.01
O2	Octopus (inside the head)	++	1.32
O3	Octopus (inside the vitreous sac of the eyes)	+++	1.5
Sp4	Sepia (inside the vitreous sac of the eyes)	+++	1.41
Sp5	Sepia (the feeding tentacles)	+++	1.49
Sp6	Sepia (fins)	+	1.13
Sh7	Shrimp	++	1.28
Sq8	Squid (inside the vitreous sac of the eyes)	+++	1.45
Sq9	Squid (fins)	+	1.04
Sq10	Squid (dorsal)	+	1.1
Sq11	Squid (the feeding tentacles)	+++	1.42
Cj12	Comb jelly	++	1.25

Degree of bioluminescence: strong (+++), medium (++), and weak (+)

**Phenotypic and bioluminescence characterization of the selected strain**

*Vibrio* sp. 6EFE exhibited creamy round colonies on LA medium and turned brown as the culture becomes old. The cell morphology characteristics showed Gram-negative, with aerobic growth conditions. In addition, it appeared straight to curved non-sporulating rods with approximately 0.6 to 0.7 μm in width and 1.2 to 2.4 μm in length as shown in Fig. 2A. It grew well at the temperature range of 15-25°C, in the presence of 3-6%

NaCl, and pH 7.0. For biochemical characteristics, it was positive to glucose, lactose, maltose, and methyl red tests. In addition, it was positive to indole test, gelatin hydrolysis, citrate utilization, catalase, oxidase, beta-glucosidase, L-proline arylamidase, and Glu-gly-arg-arylamidase tests and negative to urease test [21, 22]. For the bioluminescence feature, a bluish-green was emitted by *Vibrio* sp. 6EFE that was streaked on the LA plate and detected in a dark room in the absence of light as shown in Fig. 2B.

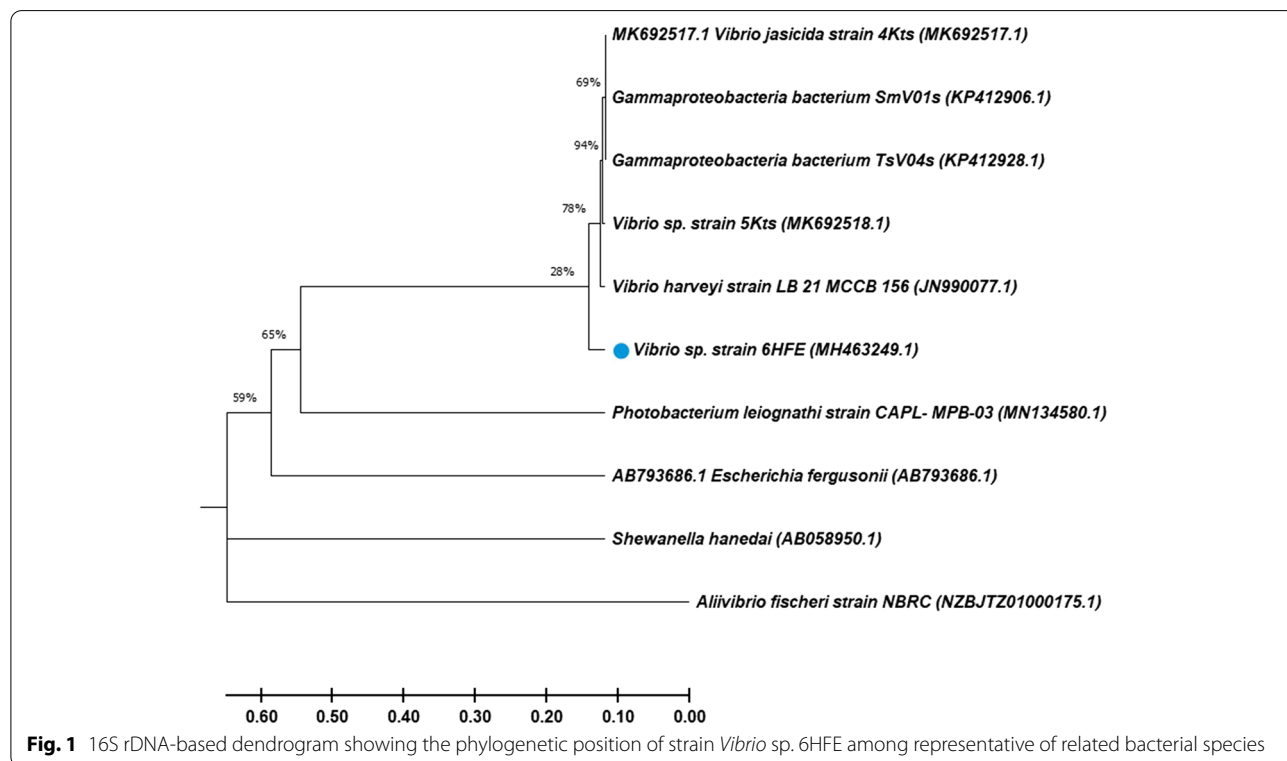


**Fig. 1** 16S rDNA-based dendrogram showing the phylogenetic position of strain *Vibrio* sp. 6HFE among representative of related bacterial species



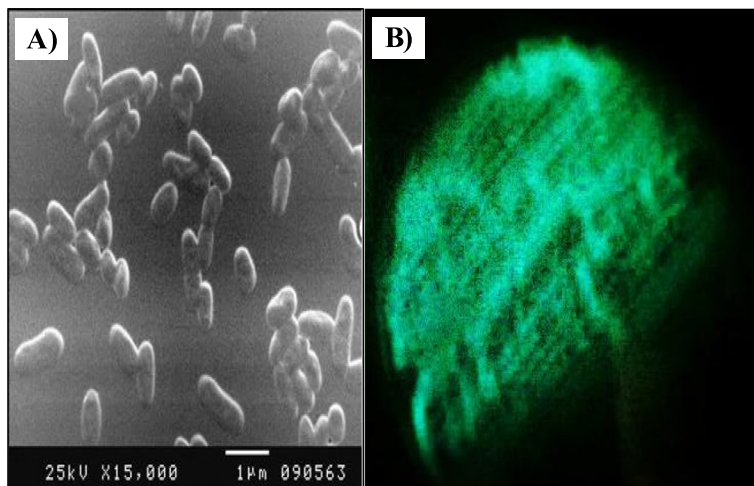


**Fig. 2** **A** SEM micrograph of *Vibrio* sp. 6EFE (x15,000); **B** bioluminescence of *Vibrio* sp. 6HFE grown on LA medium agar plates for 12 h at 30°C

**Bioluminescence intensity optimization**

*One variable at a time (OVAT)* Three variables were investigated here to study their effect on the bioluminescence of *Vibrio* sp. 6HFE. The effect of temperature is illustrated in Fig. 3A. *Vibrio* sp. 6HFE displayed high-intensity values  $1.5 \times 10^6$  and  $1.47 \times 10^6$  CPS, at 25°C and 30°C, respectively, and also high stability till 6h.

At a temperature lower or higher than this range, bioluminescence decreased greatly and was inhibited completely at  $> 30^\circ\text{C}$ . For aeration effect, the bioluminescence intensity appeared higher under shaking than static condition, at 25°C for 12 h, as illustrated in Fig. 3B. The effect of incubation time is shown in Fig. 3C, and the bioluminescence intensity curve of *Vibrio* sp. 6HFE in association with the growth curve was studied at a fixed time

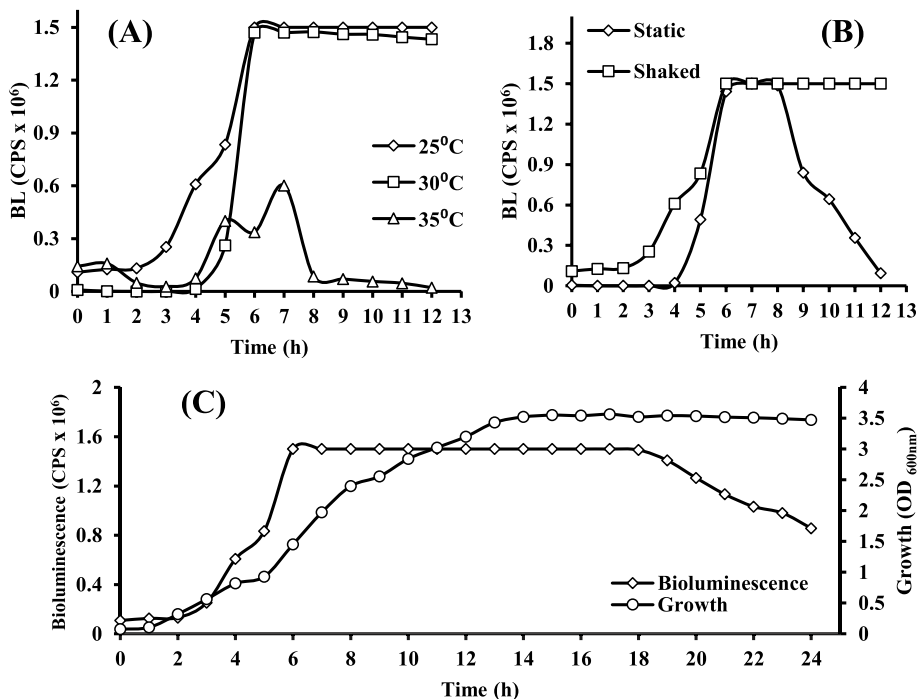


**Fig. 3** Bioluminescence of *Vibrio* sp. 6HFE grown on LA broth at different temperatures (A), under shaken and static conditions (B), and correlation between bioluminescence of *Vibrio* sp. 6HFE and its growth (C)

interval over 24 h of incubation, under shaking condition at 25°C. A typical growth profile with characteristic stages (lag, logarithmic, and stationary) was displayed. In parallel, the bioluminescence intensity increased steadily till reached to its maximum value  $1.5 \times 10^6$  CPS at the stationary phase. However, upon 24-h incubation, the bioluminescence intensity remained stable.

Statistical experimental design

- Plackett-Burman design

In this study, the most significant independent parameters for maximum bioluminescence intensity were defined via PBD, which showed variation that ranged from  $0.12 \times 10^6$  CPS (trial number 6) to  $1.39 \times 10^6$  CPS (trial number 3) (Table 4). Such result disparities implied the decisive role of the optimization process in maximizing light intensity. The analysis of multiple linear regression coefficients of the model was performed by applying MINITAB 14 by Student's *t*-test. Through using Student's *t*-test, the error mean square was calculated in order to check the significance of the estimated coefficient of the regression equation. The variable considered as significant when its confidence level (%) is higher than 95% ( $\text{prop} > F < 0.05$ ) [23, 24]. Thus, the most significant variables influencing the bioluminescence of *V. sp.* 6HFE were  $\text{MgSO}_4$ ,  $\text{K}_2\text{HPO}_4$ ,  $\text{CaCl}_2$ , and yeast extract with confidence levels of 99.6%, 97%, 97.8%, and 97.7%, respectively (Table 5).

Moreover, the Pareto chart elucidated the arrangement of the examined variables affecting light intensity in descending order (Fig 4), where the vertical red line in the chart represents a *T*-value of 3.182 that indicates the

least statistically significant influence for 95% confidence level. The other insignificant variables did not override the *T*-value (red line). The standard analysis of variance ANOVA of PBD clarified that the model was significant as indicated by the low probability value [*P*-value = 0.024] (Table 6). Furthermore, the overall fitting of the model was tested by evaluation of the coefficient of determination ( $R^2$ ) and the adjusted- $R^2$  (adj- $R^2$ ) value, which should be in reasonable agreement with the  $R^2$  value (less than 2%) [25, 26]. However, a more accurate model with higher prediction of response conjugates with an  $R^2$  value closer to 1 [24]. In our study, the model  $R^2$  and adj- $R^2$  values recorded 0.9758 and 0.9112, respectively. Such results indicate that 97.58% of the variability of the data can be explained by the model, and there is only a 2.42% chance, which could be due to noise.

The first-order model for bioluminescence intensity obtained by ANOVA was fitted to the results obtained from the 12-experiment matrix, which indicated the response (bioluminescence intensity) as a function of eight studied parameters (Eq. 6).

$$Y(\text{BL}) = 465552 - 22323 \text{ pH} + 9227 \text{ glycerol} - 127123 \text{ yeast} + 10994 \text{ peptone} + 30886 \text{ NaCl} + 128397 \text{ CaCl}_2 + 239879 \text{ MgSO}_4 - 115497 \text{ K}_2\text{HPO}_4 \tag{6}$$

For the subsequent stage of optimization (central composite design CCD), all parameters with a positive influence on response were remained constant at their high level, and those parameters negatively influenced were fixed at their low level.

- Central composition design (CCD)

**Table 4** PBD matrix to evaluate the significant variables affecting BL intensity

Run order	pH	Glycerol	Yeast	Peptone	NaCl	CaCl <sub>2</sub>	MgSo <sub>4</sub>	K <sub>2</sub> HPO <sub>4</sub>	BL intensity (CPS) × 10 <sup>6</sup>	
									Experimental	Predicted
1	1	1	-1	1	-1	-1	-1	1	0.15	0.08
2	-1	1	1	1	-1	1	1	-1	1.13	1.08
3	1	-1	-1	-1	1	1	1	-1	1.39	1.31
4	-1	-1	1	1	1	-1	1	1	0.43	0.39
5	1	1	-1	1	1	-1	1	-1	1.02	1.10
6	-1	1	1	-1	1	-1	-1	-1	0.12	0.14
7	1	-1	1	1	-1	1	-1	-1	0.24	0.29
8	1	1	1	-1	1	1	-1	1	0.13	0.12
9	-1	-1	-1	1	1	1	-1	1	1.38	1.42
10	-1	1	-1	-1	-1	1	1	1	1.04	1.09
11	-1	-1	-1	-1	-1	-1	-1	-1	0.32	0.31
12	1	-1	1	-1	-1	-1	1	1	0.22	0.26

**Table 5** Statistical analysis of PBD for BL of *V. sp. 6HFE*

Term	Effect	Co-ef	SE Co-ef	T-value	P-value	Confidence level (%)
Constant		465552	29508	15.78	0.001	99.9
pH	-44646	-22323	29508	-0.76	0.504	49.6
Glycerol	18454	9227	29508	0.31	0.775	22.5
Yeast extract	-254247	-127123	29508	-4.31	0.023	97.7
Peptone	21988	10994	29508	0.37	0.734	26.6
NaCl	61772	30886	29508	1.05	0.372	62.8
CaCl <sub>2</sub>	256794	128397	29508	4.35	0.022	97.8
MgSO <sub>4</sub>	479758	239879	29508	8.13	0.004	99.6
K <sub>2</sub> HPO <sub>4</sub>	-230995	-115497	29508	-3.91	0.030	97
<i>R</i> -Sq = 97.58%				<i>R</i> -Sq(adj) = 91.12%		

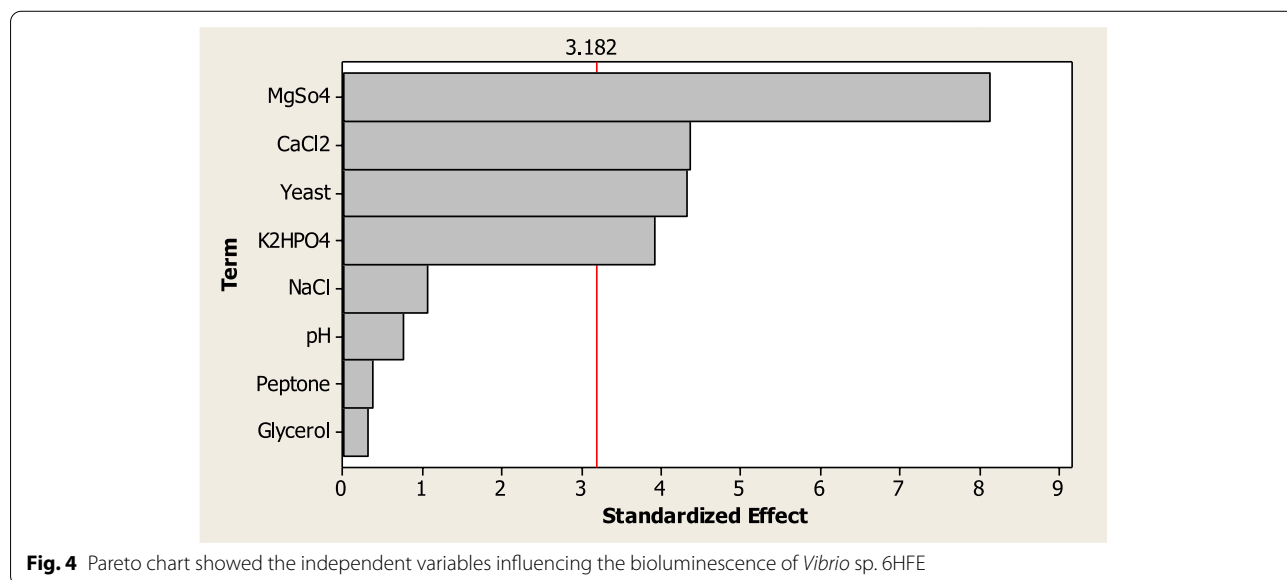


**Fig. 4** Pareto chart showed the independent variables influencing the bioluminescence of *Vibrio sp. 6HFE*

**Table 6** ANOVA for a quadratic model of BL for *V. sp. 6HFE*

Source	DF	Seq.S.S	Adj.S.S	Adj.M.S	F	P-value
Main effects	8	1.26223E+12	1.26223E+12	1.57779E+11	15.10	0.024
Residual error	3	31345296192	31345296192	10448432064		
Total	11	1.29358E+12				

To obtain the optimum response (bioluminescence intensity), CCD is an ideal technique that was used to predict exactly the most effective concentration values of the significant variables [27]. It consisted of five levels (-α, -1, 0, +1, +α) with 4 independent variables which were yeast extract, MgSO<sub>4</sub>, K<sub>2</sub>HPO<sub>4</sub>, and CaCl<sub>2</sub> for *Vibrio sp. 6HFE*. About 31 trials were performed with their response, and they included 7 replicates of central points, 16 factorial (cubic points), and 8 axial (star point) as the risk of missing non-linear

relationships has to be minimized in the middle of the intervals. The repetition is important to calculate the confidence intervals [28]. Table 7 represents different combinations of examined significant parameters in the matrix along with the actual and predicted response. As illustrated, bioluminescence intensity varied among the examined trials displaying maximum response with 1.50 × 10<sup>6</sup> CPS at trial 16 (axial point) and minimum response with 0.02 × 10<sup>6</sup> CPS at trial 14 (factorial point).



**Table 7** CCD matrix of variables influencing *V. sp.* 6HFE BL intensity

Run	Yeast	MgSO <sub>4</sub>	CaCl <sub>2</sub>	K <sub>2</sub> HPO <sub>4</sub>	BL intensity (CPS) × 10 <sup>6</sup>	
					Experimental	Predicted
1	0	0	0	0	1.45	1.36
2	-1	1	-1	1	0.30	0.42
3	1	1	1	1	0.62	0.77
4	0	2	0	0	1.25	1.09
5	0	0	0	0	1.18	1.36
6	1	-1	1	-1	0.59	0.49
7	1	1	-1	-1	0.99	1.13
8	-1	-1	-1	1	1.30	1.25
9	1	1	1	-1	0.79	0.90
10	-2	0	0	0	0.14	0.27
11	1	-1	-1	1	0.04	0.21
12	-1	1	1	-1	0.38	0.23
13	-1	-1	1	-1	1.46	1.55
14	-1	1	1	1	0.02	0.09
15	0	0	0	0	1.15	1.36
16	0	0	-2	0	1.50	1.44
17	-1	-1	1	1	1.49	1.37
18	0	0	0	0	1.49	1.36
19	1	-1	1	1	0.25	0.32
20	0	0	0	2	0.25	0.10
21	0	0	0	0	1.36	1.36
22	1	-1	-1	-1	0.28	0.26
23	-1	-1	-1	-1	1.43	1.31
24	0	0	0	0	1.39	1.36
25	0	0	2	0	1.35	1.33
26	0	0	0	-2	0.21	0.29
27	0	0	0	0	1.49	1.36
28	1	1	-1	1	1.14	1.11
29	2	0	0	0	0.11	0.10
30	0	-2	0	0	1.42	1.50
31	-1	1	-1	-1	0.46	0.45

- Statistical analysis of the data

Table 8 indicates the multiple regression analysis of the data, coefficients, *P*-value, and *F*-value. The model determination coefficient (*R*<sup>2</sup>) of 95.3% referred to the goodness of fit for the model (Table 8). The adjusted *R*<sup>2</sup> value recorded 91.2% pointing out to the high efficiency and significance. Besides, data were judged based on the significance (*P* < 0.05).

Statistical analysis of the data manifested that the model is significant, as demonstrated by a very low *P*-value (0.00 < 0.05) (Table 9). It is clear from the significance values that the linear coefficients of yeast extract, MgSO<sub>4</sub>, and quadratic effects of yeast extract and K<sub>2</sub>HPO<sub>4</sub> are significant (Table 8). The *P*-values pointed out that the

linear coefficient of CaCl<sub>2</sub> and K<sub>2</sub>HPO<sub>4</sub> was not significant (*P*-value = 0.440 and 0.173, respectively), whereas the majority of interactions between the studied variables were not significant, except yeast extract and MgSO<sub>4</sub> and CaCl<sub>2</sub> and MgSO<sub>4</sub> (*P*-values of 0.00 and 0.013, respectively), implying that they did not contribute significantly to the maximization of response. However, an additional factor that considers being a determinant for estimating the quality of the model is the lack of fit. It characterizes the variation in the data around the fitted design testified.

The insignificant lack of fit ensures a good design; it indicated that there might be contributions in the regresses-response relationship, which are not considered by the design [29]. Insignificant lack of fit is

**Table 8** Determination regression coefficient of second-order polynomial model for *Vibrio* sp. 6HFE bioluminescence

Term	Coef.	SE Coef.	T-value	P-value
Constant	1356954	62059	21.866	0.000
Yeast extract	-92777	33516	-2.768	0.014
MgSO <sub>4</sub>	-102822	33516	-3.068	0.007
CaCl <sub>2</sub>	-26553	33516	-0.792	0.440
K <sub>2</sub> HPO <sub>4</sub>	-47855	33516	-1.428	0.173
Yeast extract* yeast extract	-317865	30705	-10.352	0.000
MgSO <sub>4</sub> *MgSO <sub>4</sub>	-15062	30705	-0.491	0.630
CaCl <sub>2</sub> *CaCl <sub>2</sub>	7473	30705	0.243	0.811
K <sub>2</sub> HPO <sub>4</sub> *K <sub>2</sub> HPO <sub>4</sub>	-291506	30705	-9.494	0.000
Yeast extract *MgSO <sub>4</sub>	431849	41048	10.521	0.000
Yeast extract *CaCl <sub>2</sub>	-4030	41048	-0.098	0.923
Yeast extract *K <sub>2</sub> HPO <sub>4</sub>	1241	41048	0.030	0.976
MgSO <sub>4</sub> *CaCl <sub>2</sub>	-114325	41048	-2.785	0.013
MgSO <sub>4</sub> *K <sub>2</sub> HPO <sub>4</sub>	10236	41048	0.249	0.806
CaCl <sub>2</sub> *K <sub>2</sub> HPO <sub>4</sub>	-28726	41048	-0.700	0.494

R-Sq = 95.3% R-Sq(adj) = 91.2%

required, and herein, it recorded 0.308. To evaluate the correlation between the tested four parameters and to calculate the highest light intensity corresponding to the optimal values of yeast extract, CaCl<sub>2</sub>, MgSO<sub>4</sub>, and K<sub>2</sub>HPO<sub>4</sub>, the equation of the second-order polynomial model (Eq. 7) has been suggested. Based on the optimum levels of the independent parameters, the maximum bioluminescence intensity was predictable:

$$\begin{aligned}
 Y(\text{BL}) = & 1356954 - 92777 \text{ yeast extract} - 102822 \\
 & \text{MgSO}_4 - 26553 \text{ CaCl}_2 - 47855 \\
 & \text{K}_2\text{HPO}_4 - 317865 \text{ yeast extract} * \text{yeast extract} - 15062 \\
 & \text{MgSO}_4 * \text{MgSO}_4 + 7473\text{CaCl}_2 * \text{CaCl}_2 - 291506 \\
 & \text{K}_2\text{HPO}_4 * \text{K}_2\text{HPO}_4 + 431849 \text{ yeast extract} * \\
 & \text{MgSO}_4 - 4030 \text{ yeast extract} * \text{CaCl}_2 + 1241 \text{ yeast extract} * \\
 & \text{K}_2\text{HPO}_4 - 114325 \text{ MgSO}_4 * \text{CaCl}_2 + 10236 \\
 & \text{MgSO}_4 * \text{K}_2\text{HPO}_4 - 28726\text{CaCl}_2 * \text{K}_2\text{HPO}_4
 \end{aligned}$$

(7)

For checking the accuracy of the model, normal probability plot and residual plots were evaluated. The normal

probability plot is a useful graphical method to characterize the nature of the residuals and validate models (Fig. 5). All residuals are close to the diagonal line in a way that indicates they are normally distributed. In the residual plots, all residuals are randomly and uniformly scattered against the fitted values of the model. Therefore, all previous evidence reflects a good model fit and affirms the model's adequacy.

- Graphical plots for interaction effect representation

The three-dimensional surface and two-dimensional contour plots were designed to illustrate the interaction effect between response (bioluminescence intensity) and examined independent parameters, besides identifying and predicting the optimal concentrations for maximal response. As observed in Fig. 6A, bioluminescence intensity was plotted on the Z-axis against yeast extract and MgSO<sub>4</sub>, while the other factors were set at their zero level. It showed that when concentrations of both variables decreased, the bioluminescence intensity gradually

**Table 9** ANOVA of the quadratic polynomial model for BL of *Vibrio* sp. 6HFE

Source	DF	Seq SS	Adj SS	Adj MS	F	P
Regression	14	8.71958E+12	8.71958E+12	6.22827E+11	23.10	0.000
Linear	4	5.32199E+11	5.32199E+11	1.33050E+11	4.94	0.009
Square	4	4.97921E+12	4.97921E+12	1.24480E+12	46.17	0.000
Interaction	6	3.20818E+12	3.20818E+12	5.34696E+11	19.83	0.000
Residual error	16	4.31349E+11	4.31349E+11	26959290759		
Lack-of-fit	10	3.10610E+11	3.10610E+11	31060968406	1.54	0.308
Pure error	6	1.20739E+11	1.20739E+11	20123161346		
Total	30	9.15093E+12				

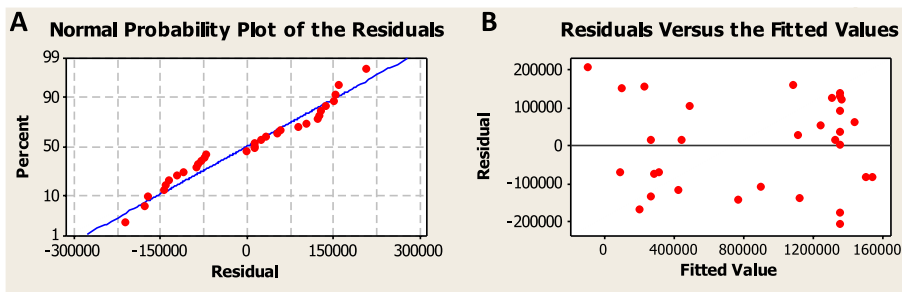


**Fig. 5** A Normal probability plot of residuals against bioluminescence, B residual distribution against fitted values plot of RSM

increased. The saddle contour plot (Fig. 6B) reflected the significant synergistic interaction between them. Generally, the shape of the contour plot reveals the nature and extent of the interactions between the variables. However, a circular contour plot highlights an insignificant interaction between variables [27, 30]. Consequently, the correlation between yeast extract and  $K_2HPO_4$  could be described as insignificant, as indicated by the circular 2D-contour plot (Fig. 6D). Furthermore, at the moderate level of both factors, the highest response is obtained in Fig. 6C. However, the antagonistic correlation could describe the interaction effect of  $MgSO_4$  and  $CaCl_2$  (Fig. 6E), where the maximum bioluminescence intensity could be achieved by increasing the concentration of  $CaCl_2$  and decreasing  $MgSO_4$  concentration or vice versa (Fig. 6F).

To attain maximum bioluminescence, the response optimizer tool in MINITAB 14 was applied by solving the reduced regression models. This tool calculates the individual desirability using a transfer or desirability function. As the composite desirability reached its maximum, the optimal response was obtained. Always, the response optimizer is between zero and one. When it equals one, it means that the response (bioluminescence intensity) becomes at the ideal case. But when it equals zero, it indicates that the response is outside agreeable limits. The response optimizer at optimum conditions for maximum targets is shown in Fig. 7.

The desirability value for *V. sp.* 6HFE is 1.0, confirming the fitting of the performed design that results in maximum bioluminescence ( $1.5 \times 10^6$  CPS). The optimum predicted concentrations (g/L) of the significant variables

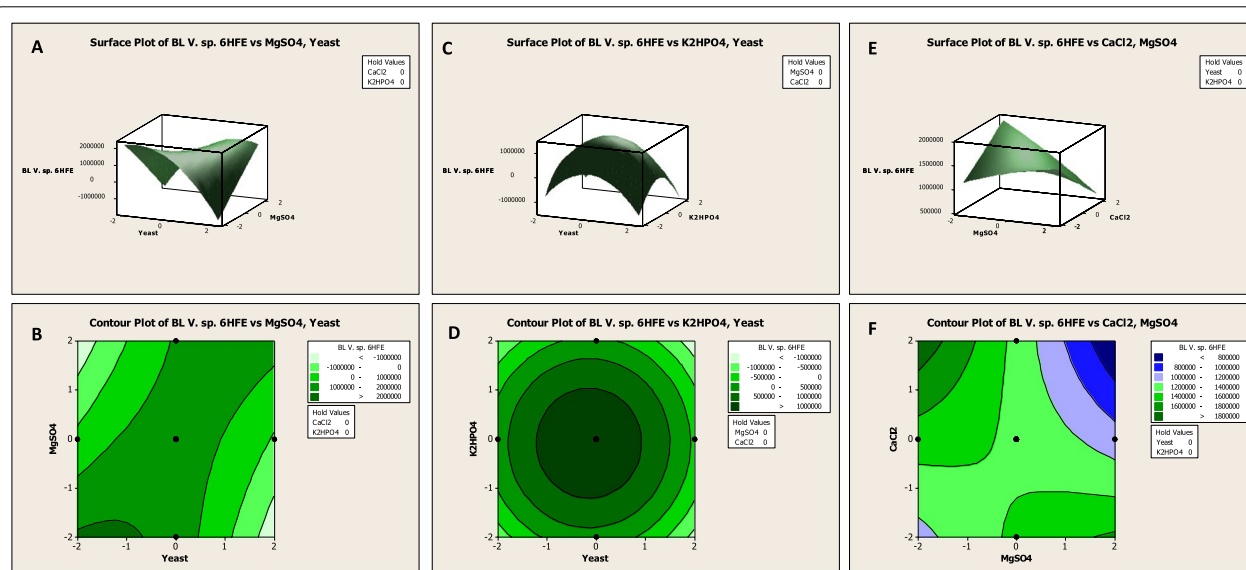


**Fig. 6** 3D surface plot (left panels) and 2D contour plot (right panels) displaying the mutual effects of independent significant variables on bioluminescence intensity

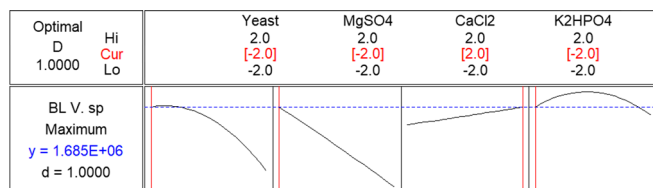


**Fig. 7** Response optimizer and desirability function of *V. sp.* 6HFE bioluminescence

for *V. sp.* 6HFE were yeast extract, 0.2; CaCl<sub>2</sub>, 4.0; MgSO<sub>4</sub>, 0.1; and K<sub>2</sub>HPO<sub>4</sub>, 0.1.

- Verification of the model

The validation of the experimental results of *V. sp.* 6HFE for bioluminescence intensity was evaluated by comparing optimum conditions predicted from CCD and basal un-optimized conditions. This optimization strategy succeeded in maximizing bioluminescence intensity within 1 h from (initial basal)  $0.66 \times 10^6$  CPS to  $1.5 \times 10^6$  CPS (predicted from CCD) by a 2.3-fold increase.

*Application of Vibrio sp. 6HFE as biosensor*

- BIA for various solvents

The toxicity effect of nine solvents with different categories, polarities, and different concentrations ranging from 0.006 to 12.3 M was tested on the bioluminescence of *Vibrio sp.* 6HFE for 5 min, the selected shortest exposure time bioassay. Based on IC<sub>50</sub> results of all examined solvents (Fig. 8),

the toxicity of the nine organic solvents could be arranged from the most toxic to the least toxic as the following: chloroform > isoamyl > acetic acid > formamide > ethyl acetate > acetonitrile > DMSO > acetone > methanol.

- BIA for heavy metals

The bioluminescence profile of *V. sp.* 6HFE in the presence of eight heavy metals was studied (Cr<sup>6+</sup>, Co<sup>2+</sup>, Cu<sup>2+</sup>, Fe<sup>2+</sup>, Hg<sup>+</sup>, Ag<sup>+</sup>, Ni<sup>2+</sup>, and Zn<sup>2+</sup>) at concentrations (1 to 1000 ppm). Obviously, silver and mercury completely inhibited the bioluminescence in all examined concentrations. The IC<sub>50</sub> values of examined heavy metals for the bioluminescence of *Vibrio sp.* 6HFE are represented in Fig. 9. Accordingly, the order of toxicity for bioluminescence of *Vibrio sp.* 6HFE could be expressed from the most toxic to the least toxic as the following: Ag<sup>+</sup> > Hg<sup>+</sup> > Zn<sup>2+</sup> > Cu<sup>2+</sup> > Cr<sup>6+</sup> > Fe<sup>6+</sup> > Co<sup>2+</sup> > Ni<sup>2+</sup>.

- BIA for aromatic hydrocarbon compounds

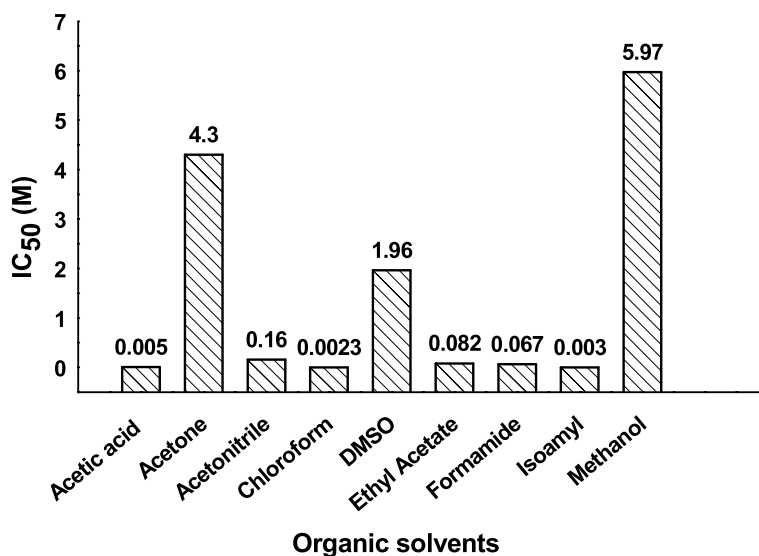


**Fig. 8.** IC<sub>50</sub> of organic solvents on the bioluminescence of *Vibrio sp.* 6HFE

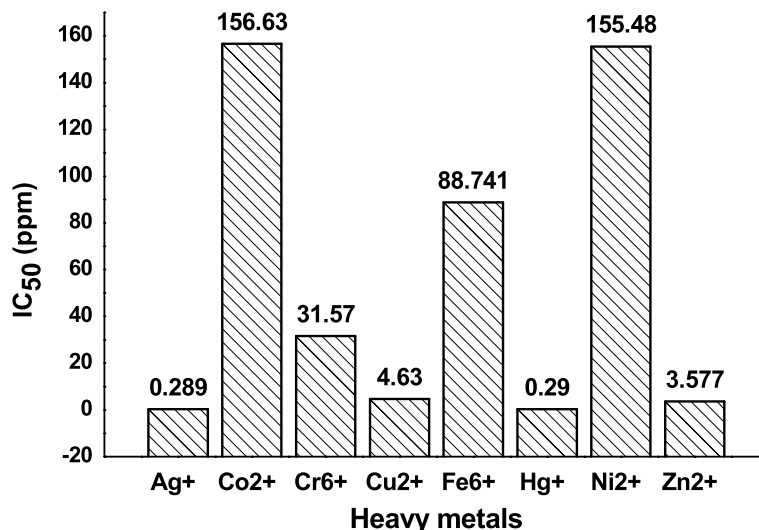


Fig. 9 IC<sub>50</sub> of heavy metals on the bioluminescence of *Vibrio* sp. 6HFE

The bioluminescence inhibition pattern of *Vibrio* sp. 6HFE in the response to hydrocarbons (benzene, catechol, phenol, and penta-chlorophenol) at concentrations (1 to 1000 ppm) was evaluated for 5 min. The IC<sub>50</sub> values of them are demonstrated in Fig. 10. The bioluminescence of *Vibrio* sp. 6HFE was inhibited by benzene, catechol, phenol, and penta-chlorophenol at 443.1, 500, 535.1, and 537.4 ppm. Therefore, the toxicity order of them was arranged from the most toxic to the least toxic as the following: benzene > catechol > phenol > penta-chlorophenol.

- BIA for polluted samples

The biosensor *V. sp.* 6HFE was employed for pollution detection in four different real ecosystems: two samples from industrial effluents and two others from polluted seawater (El-Dekheila and El-Max). The following Fig. 11 illustrates the bioluminescence inhibition (%) as a result of the exposure of *V. sp.* 6HFE to real polluted samples. As noticed, the effluent of AKSA Company resulted in 93% of bioluminescence inhibition implying a higher pollution percentage. However, the bioluminescence inhibition was displayed by 54%, 52%, and 45% for El-Dekheila’s seawater, Tiba’s Company, and El-Max seawater, respectively. Notably, the chemical analysis of examined samples revealed higher pollution with various heavy

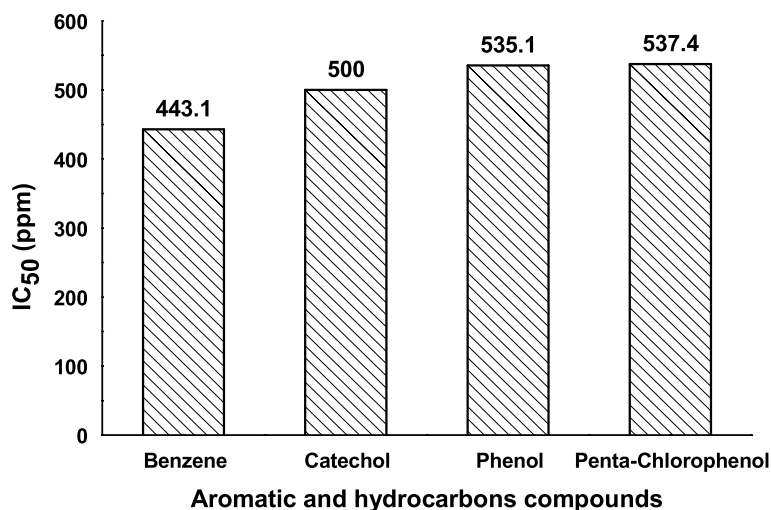


Fig. 10 IC<sub>50</sub> of aromatic and hydrocarbon compounds on the bioluminescence of *Vibrio* sp. 6HFE



metals where AKSA contained  $Zn^{2+} \approx 2.4$  ppm and  $Fe^{2+} \approx 0.54$ , Dekhila sample recorded  $Cr^{6+}$  0.51 ppm and  $Fe^{2+}$  0.39 ppm, and Tiba and El-Max samples had 0.6 and 0.38 ppm of  $Fe^{2+}$ . However, Environmental Pollution and Legislative Regulations (Law 48. 1982 & Decree 8, 1993) of Egypt stated that the allowable limit of  $Zn^{2+}$  and  $Cr^{6+}$  must not exceed 1.0 and 0.01–0.05 ppm, respectively.

## Discussion

Several studies reported light emission from *V. fischeri*, *V. harvei*, *V. parahaemolyticus*, *V. alginolyticus*, and *V. vulnificus* [31, 32]. Many literatures assured the symbiotic relationship between the common cuttlefish (*Sepia officinalis*) and the bioluminescent *Vibrio* species [33–35]. The isolated bacterial strain from *Sepia* belongs to the genus *Vibrio* and deposited in GenBank as *Vibrio* sp. 6HFE. It is observed that the bioluminescence of *Vibrio* sp. 6HFE was optimum at 25°C. Similarly, *V. fischeri* was able to grow and efficiently illuminated at a temperature range 20–26°C [36, 37]. Notably, the optimum temperature for luciferase was 25°C. As luciferase is temperature dependent, the bioluminescence exhibited higher intensity at the range of 25 to 30°C and fluctuated notoriously above 30°C as mentioned by [38–40].

Also, it is noted that the bioluminescence stability of *Vibrio* sp. 6HFE was raised by aeration. Such result could be explained by proper and homogenous distribution of media component and oxygen under shaking condition, where, under appropriate aeration conditions, the expression of lux operon enhances which subsequently elevates

quorum sensing. Additionally, the agitation reduces the effect of exhaust gas produced during the incubation period [39, 41]. The relationship between the increasing of bioluminescence intensity and the growth curve of *Vibrio* sp. 6HFE revealed that the stationary phase has the highest bioluminescence intensity combined with stability. In agreement with these results, Thorn et al. [42] noted that luminous *Pseudomonas aeruginosa* MCS5-lite emitted stable bioluminescence during the stationary phase. Eventually, the process of bioluminescence is time dependent which relies mostly on bacterial cell density and subsequent autoinducer accumulation [43].

Out of statistical experiment results, yeast extract had a high effect of the bioluminescence intensity at low concentrations. This could be attributed to the light-blocking effect of yeast extract upon higher concentrations, where the extremely nutritive nature of yeast extract resulted in a much higher bacterial growth rate which ultimately led to much higher cell density that is proportional to the bioluminescence as previously reported by Lee et al. and Hassan and Oh [44, 45]. Otherwise,  $Ca^{2+}$  and  $Mg^{2+}$  enhanced the bioluminescence of *V. sp.* 6HFE upon higher concentrations. Both cations act as cofactors for luciferase enzyme and in some species cofactors for photoprotein which appears in the absence of luciferase enzyme. Such chemical molecule is a combination of luciferin protein and oxygen which requires  $Ca^{2+}$  or  $Mg^{2+}$  for emitting light [46]. However,  $K^+$  improved the bioluminescence of *V. sp.* 6HFE, where it plays a special role in increasing the long-chain aldehydes and intracellular luminescent proteins and subsequently elevates the light output. Furthermore, it

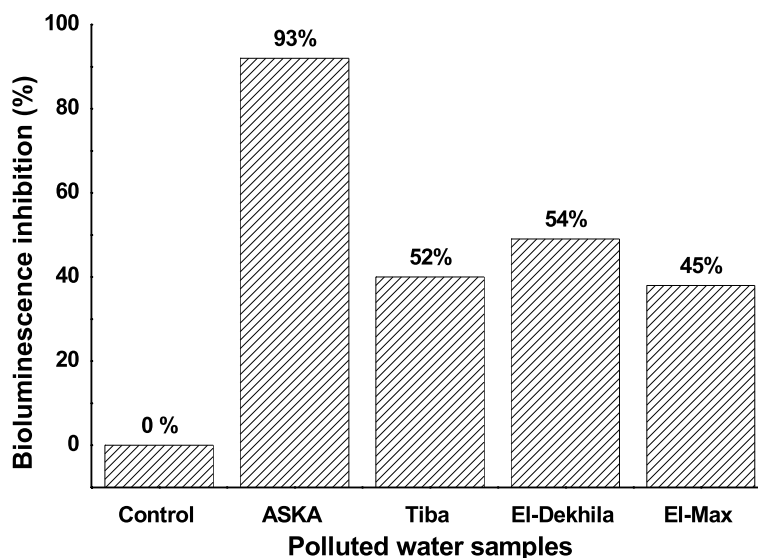


**Fig. 11** Effect of different polluted water samples on the bioluminescence of the biosensor *Vibrio* sp. 6HFE

regulates the osmolarity process through affecting on the energetics of the outer cytoplasmic membrane and consequently the intensity of bioluminescence, which is affected by changing the cell respiration rate [47, 48]. Besides that,  $K^+$  in the medium increased membrane phosphorylation and transmembrane electrochemical gradient; as a result, it stimulated more bioluminescence at acidic condition [45, 47].

The process of light emission is somehow a reflection to the bacterial metabolic and enzymatic intensity and any inhibition occurred which led to a noticeable change in the luminescence production. Therefore, it is possible to utilize such property in monitoring and estimating the toxicity of any pollutant, even at low concentrations. Generally, the bioluminescence inhibition assay (BIA) becomes one of the most popular bioassays for the evaluation of toxicity in aqueous solutions [5, 6]. Accordingly, the bioluminescent strain *Vibrio* sp. 6HFE would be applied as a biosensor for detecting pollution. The toxicity of pollutant was determined in the form of  $IC_{50}$  within a short time (5-30 min) through the BIA approach as revealed by Cukurluoglu and Muezzinoglu and Halmi et al. [19, 20]. Broadly, such monitoring bioassay considers being a simple and fast detection approach by producing an alarm in the form of light on/off. In addition, it is a clean and cost-effective method in comparison to chemical methods [49, 50]. Out of the results, it is observed that *Vibrio* sp. 6HFE was found to be characteristic by exhibiting lower  $IC_{50}$  with the tested solvents compared to other studies [51]. It is found that just 2.0 ppm of zinc and copper led to moderate inhibition of the bioluminescence intensity at only 5 min compared to *Photobacterium* sp. strains MIE and LuB-1 which recorded 0.85 and 1.08 ppm as  $IC_{50}$  for zinc and copper at 15 min, correspondingly as stated by Halmi et al. and Hong et al. [15, 52]. In comparison to the results of other literatures [53], it could be concluded the efficiency of *Vibrio* sp. 6HFE as a promising biosensor for detecting various pollutants with considerable concentrations in wastewater. Therefore, the strain *V. sp.* 6HFE seemed to be advantageous in providing fast and immediate indication about the pollution burden in examined samples and give alarm for movement to rapid solution.

## Conclusion

The present study demonstrated the isolation, identification, and characterization of luminous bacteria from Abo-qir bay, Alexandria, for the first time. The selected strain *V. sp.* 6HFE exhibited the highest bioluminescence intensity as assessed quantitatively. The cultural conditions were optimized to maximize light intensity

via OVAT, PBD, and CCD. By applying optimized conditions, the luminous *V. sp.* 6HFE was employed to detect the toxicity of various toxicants, including solvents, heavy metals, and hydrocarbons. The strain *V. sp.* 6HFE confirmed its efficiency as a biosensor for monitoring pollution in environmental real ecosystems.

## Abbreviations

BL: Bioluminescence; LA: Luminescence agar; CPS: Count per second; PBD: Plackett-Burman design; CCD: Central composite design; BIA: Bioluminescence inhibition assay; OVAT: One variable at a time.

## Acknowledgements

This research was conducted at the City of Scientific Research and Technology Applications (SRTA-City), Genetic Engineering and Biotechnology Research Institute (GEBRI), Environmental Biotechnology Department, Alexandria, Egypt, and National Institute of Oceanography and Fisheries (NIOF), Marine Environment Division, Marine Microbiology Lab., Alexandria, Egypt.

## Authors' contributions

HH proposed the research concept and design, performed the experiments, carried out the statistical analysis, analyzed and interpreted all data, and contributed substantially to the writing and revising of the manuscript. ME designed statistical experiments, interpreted statistical analysis, and contributed to the writing and revising of the manuscript. GE designed the experiments, contributed to reviewing process, and had given final approval of the version to be published. HE, SS, and HG contributed to reviewing process and had given final approval of the version to be published. All authors read and approved the final manuscript.

## Funding

This research did not receive any specific grant from funding agencies in the public, commercial, or not-for-profit sectors.

## Availability of data and materials

All data generated or analyzed during this study are included in this published article.

## Declarations

### Ethics approval and consent to participate

Not applicable

### Consent for publication

Not applicable

### Competing interests

The authors declare no competing interests.

## Author details

<sup>1</sup>National Institute of Oceanography and Fisheries (NIOF), Marine Environment Division, Marine Microbiology Lab., Kayet Bay, El-Anfushy, Alexandria, Egypt.

<sup>2</sup>City of Scientific Research and Technology Applications (SRTA-City), Genetic Engineering and Biotechnology Research Institute (GEBRI), Environmental Biotechnology Department, Alexandria, Egypt. <sup>3</sup>Botany and Microbiology Department, Faculty of Science, Alexandria University, Alexandria, Egypt.

Received: 22 November 2021 Accepted: 2 May 2022

Published online: 01 July 2022

## References

- Toriquil B, Ivan WHF (2020) Water pollution in a densely populated megapolis, Dhaka. *Water*. 12(2124):1–13. <https://doi.org/10.3390/w12082124>
- Sasakova N, Gregova G, Takacova D, Mojzisoava J, Papajova I, Venglovsky J, Szaboova T, Kovacova S (2018) Pollution of surface and ground water

- by sources related to agricultural activities. *Front Sustain Food Syst* 2(42):1–11. <https://doi.org/10.3389/fsufs.2018.00042>
3. Rasalingam S, Peng R, Koodali TR (2014) Removal of hazardous pollutants from wastewaters: applications of TiO<sub>2</sub>-SiO<sub>2</sub> mixed oxide materials. *J Nanomater*:1–43. <https://doi.org/10.1155/2014/617405>
  4. Sudarshan K (2019) Occurrence and distribution of organic and inorganic pollutants in groundwater. *Water Environ Res* 91:1001–1008. <https://doi.org/10.1002/wer.1166>
  5. Jarque S, Masner P, Klánová J, Prokeš R, Bláha L (2016) Bioluminescent *Vibrio fischeri* assays in the assessment of seasonal and spatial patterns in toxicity of contaminated river sediments. *Front Sustain Food Syst* 7(1738):1–11. <https://doi.org/10.3389/fsufs.2016.01738>
  6. Mohseni M, Abbaszadeh J, Maghool S, Chaichi M (2018) Heavy metals detection using biosensor cells of a novel marine luminescent bacterium *Vibrio sp.* MM1 isolated from the Caspian Sea. *Ecotoxicol Environ Saf* 148:555–560. <https://doi.org/10.1016/j.ecoenv.2017.11.002>
  7. Abbas M, Adil M, Ehtisham-ul-Haque S, Munir B, Yameen M, Ghaffar A, Shar AGM, Tahir A, Iqbal M (2018) *Vibrio fischeri* bioluminescence inhibition assay for ecotoxicity assessment: a review. *Sci Total Environ* 626:1295–1309. <https://doi.org/10.1016/j.scitotenv.2018.01.066>
  8. Brodl E, Winkler A, Macheroux P (2018) Molecular mechanisms of bacterial bioluminescence. *Comput Struct Biotechnol J* 16:551–564. <https://doi.org/10.1016/j.csbj.2018.11.003>
  9. Miyashiro T, Ruby GE (2012) Shedding light on bioluminescence regulation in *Vibrio fischeri*. *Mol Microbiol* 84(5):795–806. <https://doi.org/10.1111/j.1365-2958.2012.08065.x>
  10. Kulkarni SV, Kulkarni SB (2015) Isolation of bioluminescent bacteria and their application in toxicity testing of chromium in water. *Int J Curr Microbiol App Sci*. 4(10):23–32 ISSN: 2319-7706 <http://www.ijcmas.com/>
  11. Rehman ZU, Leiknes TO (2018) Quorum-Quenching bacteria isolated from Red Sea sediments reduce biofilm formation by *Pseudomonas aeruginosa*. *Front Microbiol* 9(1354):1–13. <https://doi.org/10.3389/fmicb.2018.01354>
  12. Salini R, Santhakumari S, Ravi AV, Pandia SK (2019) Synergistic anti-biofilm efficacy of undecanoic acid and auxins against quorum sensing mediated biofilm formation of luminescent *Vibrio harveyi*. *Aquaculture*. 498:162–170. <https://doi.org/10.1016/j.aquaculture.2018.08.038>
  13. Trang VTD, Hang CTT, Trinh PTH, Ngoc NTD, Khanh HHN, Van TTT (2020) Isolation of marine bacteria from sponges in the south-central coastal region of Vietnam with brown seaweed polysaccharide-degrading activities. *Vietnam J Sci Technol* 58(6A):41–51. <https://doi.org/10.15625/2525-2518/58/6A/15445>
  14. Kretzer WJ, Schmelcher M, Loessner JM (2018) Ultrasensitive and fast diagnostics of viable *Listeria* cells by CBD magnetic separation combined with A511::luxAB detection. *Viruses*. 10(626):1–13. <https://doi.org/10.3390/2Fv10110626>
  15. Halmi IEM, Kassim A, Shukor YM (2019) Assessment of heavy metal toxicity using a luminescent bacterial test based on *Photobacterium sp.* strain MIE. *Rendiconti Lincei Scienze Fisiche e Naturali*:1–13. <https://doi.org/10.1007/s12210-019-00809-5>
  16. Marwa E, Esmail E, Marwa AS, Marwa E, Amany I (2021) Statistical modeling of methylene blue degradation by yeast-bacteria consortium; optimization via agro-industrial waste, immobilization and application in real effluents. *Microb Cell Factories* 20:234. <https://doi.org/10.1186/s12934-021-01730-z>
  17. Amany I, Esmail ME, Marwa MA, Marwa FE, Marwa E (2022) Methyl orange biodegradation by immobilized consortium microspheres: experimental design approach, toxicity study and bioaugmentation potential. *Biology* 11(76):1–27. <https://doi.org/10.3390/biology11010076>
  18. Zeb B, Ping Z, Mahmood Q, Lin Q, Pervez A, Irshad M, Bilal M, Bhatti ZA, Shaheen S (2017) Assessment of combined toxicity of heavy metals from industrial wastewaters on *Photobacterium phosphoreum*T35. *Appl Water Sci* 7(4):2043–2050. <https://doi.org/10.1007/s13201-016-0385-4>
  19. Cukurluoglu S, Muezzinoglu A (2013) Assessment of toxicity in waters due to heavy metals derived from atmospheric deposition using *Vibrio fischeri*. *J Environ Sci Health C Part A* 48:57–66. <https://doi.org/10.1080/10934529.2012.707840>
  20. Halmi IEM, Jirangon H, Johari WLW, Abdul Rachman RA, Shukor YM, Syed AM (2014a) Comparison of Microtox and Xenoassay light as a near real time river monitoring assay for heavy metals. *Sci World J*:1–10. <https://doi.org/10.1155/2014/834202>
  21. Khalil AS, Amr AS, El-Hoshy MS (2014) Molecular studies on *Vibrio* species isolated from imported frozen fish. *Glob Vet* 12(6):782–789. <https://doi.org/10.5829/idosi.gv.2014.12.06.83316>
  22. Abdelaziz M, Ibrahim DM, Ibrahim AM, Abu-Elala MN, Abdel-moneam AD (2017) Monitoring of different *Vibrio* species affecting marine fishes in Lake Qarun and Gulf of Suez: phenotypic and molecular characterization. *Egypt J Aquat Res* 1–6. <https://doi.org/10.1016/j.ejar.2017.06.002>
  23. Zhao A, Chen F, Ning C, Wu H, Song H, Wu Y, Chen R, Zhou K, Xu X, Lu Y, Gao J (2017) Use of real-time cellular analysis and Plackett-Burman design to develop the serum-free media for PC-3 prostate cancer cells. *PLoS One* 1–16. <https://doi.org/10.1371/journal.pone.0185470>
  24. Abu-Elreesh G, El-shall H, Eltarahony M, Abdelhaleem D (2019) Conversion of cost-effective agricultural wastes into valued oil using the fungus *Curvularia Sp.*: isolation, optimization and statistical analysis. *Biosci Res* 16(3):3006–3024
  25. Alshabani A, Yaakob Z, Alsobaai A, Sahri M (2014) Optimization of Pd-β/γ Al<sub>2</sub>O<sub>3</sub> catalyst preparation for palm oil hydrogenation response surface methodology (RSM). *Braz J Chem Eng* 31:69–78. <https://doi.org/10.1590/S0104-66322014000100008>
  26. Wang X, Qu R, Wei Z, Yang X, Wang Z (2014a) Effect of water quality on mercury toxicity to *Photobacterium phosphoreum*: model development and its application in natural waters. *Ecotoxicol Environ Saf* 104:231–238. <https://doi.org/10.1016/j.ecoenv.2014.03.029>
  27. Eltarahony M, Zaki S, Abd-El-Haleem D (2020) Aerobic and anaerobic removal of lead and mercury via calcium carbonate precipitation mediated by statistically optimized nitrate reductases. *Sci Rep* 10(4029):1–20 <https://www.nature.com/articles/s41598-020-60951-1>
  28. De Lima JBC, Coelho FL, Contiero J (2010) The use of response surface methodology in optimization of lactic acid production: focus on medium supplementation, temperature, and pH control. *Biotechnology*. 48(2):175–181 <http://www.ftb.com.hr/48/48-175.html>
  29. Patel S, Kothari D, Goyal A (2011) Enhancement of dextransucrase activity of *Pediococcus pentosaceus* SPAm1 by response surface methodology. *Indian J Biotechnol* 10:346–351 <http://hdl.handle.net/123456789/12115>
  30. El Tarahony M, Zaki S, Kheiralla Z, Abd-El-Haleem D (2016) Biogenic synthesis of iron oxide nanoparticles via optimization of nitrate reductase enzyme using statistical experimental design. *Biotechnol Adv* 5(2):667–684. <https://doi.org/10.24297/jbt.v5i2.1575>
  31. Lo H, Lin J, Chen Y, Chen C, Shao C, Lai Y, Hor L (2011) RTX toxin enhances the survival of *Vibrio vulnificus* during infection by protecting the organism from phagocytosis. *J Infect Dis* 203:1866–1874. <https://doi.org/10.1093/infdis/jir070>
  32. Bjelland MA, Johansen R, Brudal E, Hansen H, Winther-Larsen CH (2012) *Vibrio salmonicida* pathogenesis analyzed by experimental challenge of Atlantic salmon (*Salmo salar*). *Microb Pathog* 52:77–84. <https://doi.org/10.1016/j.micpath.2011.10.007>
  33. Gokhale T, Wali A, Parikh S, Sood N (2012) Research of marine isolates in development of biosensors for environmental pollutants. *Eng Rev* 32(1):17–22 <https://hrcak.srce.hr/78565>
  34. Naguit AAM, Plata CK, Abisado GR, Calugay JR (2014) Evidence of bacterial bioluminescence in a Philippine squid and octopus hosts. *AAAL Bioflux* 7(6):497–507 Corpus ID: 83838088
  35. Hendry AT, Wet RJ, Dougan EK, Dunlap VP (2016) Genome evolution in the obligate but environmentally active luminous symbionts of flashlight fish genome. *GBE*. 8(7):2203–2213. <https://doi.org/10.1093/gbe/evw161>
  36. Scheerer S, Gomez F, Lloyd D (2006) Bioluminescence of *Vibrio fischeri* in continuous culture: optimal conditions for stability and intensity of photoemission. *J Microbiol Methods* 67(32):1–329. <https://doi.org/10.1016/j.mimet.2006.04.010>
  37. Abdel-hamid AA, Blaghen M (2013) Optimization of bioluminescence of *Vibrio fischeri* and assessment of Hg<sup>++</sup>, Cd<sup>++</sup>, As<sup>++</sup>, Zn<sup>++</sup>, Ag<sup>+</sup>, Cu<sup>++</sup> and Ni<sup>++</sup> ions. *Asian J Biotechnol Bioresour*. <https://doi.org/10.3390/2Fijms140816386>
  38. Wanga G, Shena H, Conga W (2006) Temperature-modulated bioluminescence tomography. *Opt Express* 14(17):7852–7871. <https://doi.org/10.1364/OE.14.007852>

39. Zhou Y, Han L, He H, Sang BYD, Feng J, Zhang X (2018) Effects of agitation, aeration and temperature on production of a novel glycoprotein GP-1 by *Streptomyces kanasensis* ZX01 and scale-up based on volumetric oxygen transfer coefficient. *Molecules*. 23(1):1–14. <https://doi.org/10.3390/molecules23010125>
40. Williams FC, Geroni MG, Lloyd D, Choi H, Clark N, Pirog A, Lees J, Porcha A (2019) Bioluminescence of *Vibrio fischeri*: bacteria respond quickly and sensitively to pulsed microwave electric (but not magnetic) fields. *J Biomed Opt* 24(5):1–11. <https://doi.org/10.1117/1.JBO.24.5.051412>
41. Chavez-Dozal A, Nishiguchi KM (2011) Variation in biofilm formation among symbiotic and free-living strains of *Vibrio fischeri*. *J Basic Microbiol* 51:452–458. <https://doi.org/10.1002/jobm.201000426>
42. Thorn MSR, Nelson MS, Greenman J (2007) Use of a bioluminescent *Pseudomonas aeruginosa* strain within an in vitro microbiological system, as a model of wound infection, to assess the antimicrobial efficacy of wound dressings by monitoring light production. *Antimicrob Agents Chemother* 51(9):3217–3224. <https://doi.org/10.1128/aac.00302-07>
43. Lin YL, Meighen AE (2009) Bacterial bioluminescence: biochemistry and molecular biology. *Photochem Photobiol Sci* <http://photobiology.info/>
44. Lee B, Lee J, Shin D, Kim E (2001) Statistical optimization of bioluminescence of *Photobacterium phosphoreum* KCTC2852. *J Biosci Bioeng* 92(1):72–76. <https://doi.org/10.1263/jbb.92.72>
45. Hassan HAS, Oh ES (2010) Improved detection of toxic chemicals by *Photobacterium phosphoreum* using modified Boss medium. *J Photochem Photobiol B Biol* 101:16–21. <https://doi.org/10.1016/j.jphotobiol.2010.06.006>
46. Homaei AA, Myramdi BA, Sariri R, Kamrani E, Stevanato R, Etehad S, Khajeh K (2013) Purification and characterization of a novel thermostable luciferase from *Benthosema pterotum*. *J Photochem Photobiol B Biol* 125:131–136. <https://doi.org/10.1016/j.jphotobiol.2013.05.015>
47. Deryabin GD, Aleshina SE (2008) Effect of salts on luminescence of natural and recombinant luminescent bacterial. *Appl Biochem Microbiol* 44(3):292–296. <https://doi.org/10.1134/S0003683808030113>
48. Tabei Y, Era M, Ogawa A, Morita H (2011) Effects of magnesium sulfate on the luminescence of *Vibrio fischeri* under nutrient-starved conditions. *Biosci* 75(6):1073–1078. <https://doi.org/10.1271/bbb.100880>
49. Parvez S, Venkataraman C, Mukherji S (2006) A review on advantages of implementing luminescence inhibition test (*Vibrio fischeri*) for acute toxicity prediction of chemicals. *Environ Int* 32(2):265–268. <https://doi.org/10.1016/j.envint.2005.08.022>
50. Girotti S, Ferri NE, Fumo MG, Maiolini E (2008a) Monitoring of environmental pollutants by bioluminescent bacteria. *Anal Chim Acta* 608:2–29. <https://doi.org/10.1016/j.aca.2007.12.008>
51. Blaschke U, Paschke A, Rensch I, Schuurmann G (2010) Acute and chronic toxicity toward the bacteria *Vibrio fischeri* of organic narcotics and epoxides: structural alerts for epoxide excess toxicity. *Chem Res Toxicol* 23:1936–1946. <https://doi.org/10.1021/tx100298w>
52. Hong Y, Chen Z, Zhang B, Zhai Q (2010) Isolation of *Photobacterium* sp. LuB-1 and its application in rapid assays for chemical toxicants in water. *Lett Appl* 51:308–312. <https://doi.org/10.1111/j.1472-765x.2010.02896.x>
53. Repetto G, Jos A, Hazen JM, Molero LM, del Peso A, Salguero M, del Castillo P, Rodriguez-Vicente MC, Repetto M (2001) A test battery for the ecotoxicological evaluation of pentachlorophenol. *Toxicol*. 15:503–509. [https://doi.org/10.1016/s0887-2333\(01\)00055-8](https://doi.org/10.1016/s0887-2333(01)00055-8)

## Publisher's Note

Springer Nature remains neutral with regard to jurisdictional claims in published maps and institutional affiliations.

Submit your manuscript to a SpringerOpen<sup>®</sup> journal and benefit from:

- Convenient online submission
- Rigorous peer review
- Open access: articles freely available online
- High visibility within the field
- Retaining the copyright to your article

---

Submit your next manuscript at ► [springeropen.com](https://www.springeropen.com)

---